Journal of Engineering Mechanics and Machinery (2024)
Clausius Scientific Press, Canada

DOI: 10.23977/jemm.2024.090206
ISSN 2371-9133 Vol. 9 Num. 2

Development and Performance Evaluation of a Double-Grating Temperature-Compensated Bolt for Accurate Strain Measurement

Hao Wang[1,2,3,4,a], Nian Zhu[1,2,3,4,b], Heng Li[1,2,3,4,c,*]

[1]Institute of Seismology, CEA, Wuhan, China
[2]Hubei Key Laboratory of Earthquake Early Warning, Wuhan, China
[3]Hubei Earthquake Administration, Wuhan, China
[4]Wuhan Institute of Earthquake Engineering Co. Ltd., Wuhan, China
[a]31317120@qq.com, [b]414099406@qq.com, [c]liangyabin2006@126.com
[*]Corresponding author

Keywords: Optical Fiber Sensing Technology; Temperature-Compensated Double-Grating Bolt; Double Wavelength Matrix Method; Temperature Compensation

Abstract: Recently, the fiber Bragg grating (FBG)-based bolt has been proposed and attempted to apply to the monitoring of pit slope stability. However, the measurement performance of the FBG-embedded bolt is known to be influenced not only by strain but also by ambient temperature. This often makes it challenging, if not impossible, to obtain accurate deformation measurements of the bolt. To address this issue, this study developed a novel temperature-compensated double-grating bolt to achieve temperature compensation and accurate strain measurement. This bolt incorporates two FBG sensors installed using different techniques to achieve distinct temperature sensitivity and strain sensitivity coefficients. This unique setup successfully decouples temperature and strain effects in the host bolt by employing the double wavelength matrix method. This paper first details the decoupling principle of the developed bolt, followed by an experimental investigation into its effectiveness and feasibility for temperature compensation and strain measurement in a laboratory setting. The results confirm that the developed bolt provides a great possibility to accurately measure the strain despite significant variations in ambient temperature. This bolt shows promising potential to be used in the area of the monitoring for building structures, mining slopes, and other areas.

1. Introduction

Anchor bolt support technique is widely utilized in mining [1-2], tunnel construction [3-4], slope control, and treatment [5-6], among others. This technology significantly enhances the stability of surrounding rock and slopes, thereby preventing engineering accidents such as collapses and landslides. However, anchor bolts are affected by various factors during service, including anchoring quality, construction vibrations, earthquakes, heavy precipitation, and long-term ground pressure. These factors can induce deformation and instability in the rock and soil structure when

the changing tensile shear stress exceeds the bolt's limit state, potentially leading to failure. To monitor anchor bolts' stress and strain and grasp the ground pressure state in real time, some researchers have integrated sensors with bolt anchors to create sensing-capable load-measuring bolts. Recent advancements have seen researchers combine FBG sensing technology with bolt rods to monitor axial forces, thereby assessing the service status and health condition of the host structure. For example, Chai [7] conducted a tensile test on a bolt embedded with fiber grating and a strain gauge, comparing and analyzing the strain measurements of these sensors. The results demonstrated that the embedded FBG sensor offers superior resolution and sensitivity of the strain measurement. Meanwhile, the feasibility of the FBG-embedded anchor bolt for the monitoring has also been verified. Jiang *et al.* [8] applied an FBG sensor to a bolt to monitor axial forces, highlighting the sensor's distinguished sensing performance and its ability to overcome the limitations of resistive bolt dynamometers. Overall, the FBG-embedded bolt has been proven viable for many projects, including concrete structure reinforcement, enabling effective and long-term monitoring [9-11].

Despite these advancements, it is well known that both strain and ambient temperature can influence the measurement performance of FBG-embedded bolts, often complicating the acquisition of accurate deformations. To improve strain measurement accuracy, temperature compensation is essential to mitigate the influence of temperature on the grating's wavelength. Regrettably, many recent studies on FBG-based bolts overlook temperature compensation or require an additional temperature sensor near the bolt to measure ambient conditions [12]. Tian *et al.* [13] proposed a dual grating-based anchor bolt with one FBG sensor measuring wavelength variations caused by strain and temperature changes and another FBG sensor solely for temperature measurement. However, this configuration for the temperature measurement FBG sensor, which requires installation in an unstressed bolt area, is complicated, space-consuming, and unsuitable for construction scenes.

To address these challenges, this study introduces a novel temperature-compensated dual-grating bolt based on the dual-wavelength matrix method, enabling the effective acquisition of both temperature and strain parameters. This paper initially outlines the design and principle of the decoupling algorithm, followed by an experimental investigation of the bolt's strain and temperature measurement performance in a laboratory setting. The identification results are analyzed and compared in detail.

2. Fiber Grating Sensing and Temperature Compensation Principle

In this study, a double grating approach is employed to simultaneously measure the temperature and strain of a bolt, utilizing the double wavelength matrix method. Initially, one grating is encased within a tubular structure, modifying its temperature and strain sensitivity coefficients. The second grating remains in a bare state. This configuration significantly differs between the two gratings regarding their temperature and strain sensitivity coefficients.

Subsequently, the strain and temperature fields can be effectively decoupled by applying the following sensing equations. This method allows each grating to respond differently to the same environmental conditions, enabling precise calculations that separate the contributions of temperature and strain to the changes in the wavelength observed. This dual-grating setup enhances the accuracy and reliability of the measurements, which is crucial for applications where precise monitoring of structural integrity is required. The equations of the dual-wavelength matrix method can be referred to as follows:

$$\begin{pmatrix} \Delta\lambda_1 \\ \Delta\lambda_2 \end{pmatrix} = \begin{pmatrix} K_{T1} & K_{\varepsilon 1} \\ K_{T2} & K_{\varepsilon 2} \end{pmatrix} \begin{pmatrix} \Delta T \\ \Delta\varepsilon \end{pmatrix} \tag{1}$$

where $\Delta\lambda_1$ and $\Delta\lambda_2$ are the wavelength change of grating #1 and grating #2,respectively, K_{T1} and K_{T2} are the temperature sensitivity coefficients of grating #1 and grating #2, respectively, and $K_{\varepsilon 1}$ and $K_{\varepsilon 2}$ are the strain sensitivity coefficients of grating #1 and grating #2, respectively, ΔT and $\Delta\varepsilon$ are the temperature and strain changes, respectively.

The solution result of equation (2) is

$$\begin{cases} \Delta T = \dfrac{K_{\varepsilon 2}}{K_{T1}K_{\varepsilon 2} - K_{T2}K_{\varepsilon 1}}\Delta\lambda_1 + \dfrac{-K_{\varepsilon 1}}{K_{T1}K_{\varepsilon 2} - K_{T2}K_{\varepsilon 1}}\Delta\lambda_2 \\ \Delta\varepsilon = \dfrac{-K_{T2}}{K_{T1}K_{\varepsilon 2} - K_{T2}K_{\varepsilon 1}}\Delta\lambda_1 + \dfrac{K_{T1}}{K_{T1}K_{\varepsilon 2} - K_{T2}K_{\varepsilon 1}}\Delta\lambda_2 \end{cases} \tag{2}$$

It should be noted that the equation (2) can also be presented as follows:

$$\begin{cases} \Delta T = K_1\Delta\lambda_1 + K_2\Delta\lambda_2 \\ \Delta\varepsilon = K_3\Delta\lambda_1 + K_4\Delta\lambda_2 \end{cases} \tag{3}$$

where $K_1 = K_{\varepsilon 2}/(K_{T1}K_{\varepsilon 2} - K_{T2}K_{\varepsilon 1})$, $K_2 = -K_{\varepsilon 1}/(K_{T1}K_{\varepsilon 2} - K_{T2}K_{\varepsilon 1})$, $K_3 = -K_{T2}/(K_{T1}K_{\varepsilon 2} - K_{T2}K_{\varepsilon 1})$, $K_4 = K_{T1}/(K_{T1}K_{\varepsilon 2} - K_{T2}K_{\varepsilon 1})$

In equation (3), the temperature and strain sensitivity coefficients are the sensor's fixed coefficients after calibration. Therefore, the temperature change ΔT and strain change $\Delta\varepsilon$ can be calculated based on the wavelength changes of these two gratings, *i.e.*, the $\Delta\lambda_1$ and $\Delta\lambda_2$, which can be measured by the fiber grating demodulation instrument. It should be noted that this method requires a solution to the matrix equation, so it needs to meet the inequation, *i.e.*, $K_{T1}/K_{T2} \neq K_{\varepsilon 1}/K_{\varepsilon 2}$, and the greater the difference, the better the performance.

Compared to the single grating method, this double grating technique eliminates the need for an additional temperature sensor. Both gratings are integrated into the bolt rod during the manufacturing process. Once installed, the only requirement for operational data processing is the wavelength information collected by the fiber grating demodulation instrument. This data is then used to independently determine the stress, strain, and ambient temperature affecting the bolt rod, showcasing a streamlined and efficient approach to structural monitoring.

3. Design and Manufacture of the Double Grating Embedded Bolt

Based on the temperature compensation principle of the double grating, this study introduces a novel temperature-compensated bolt featuring a serially connected double grating. The structural composition of this innovative bolt is detailed in Figure 1.

Detailed process for the bolt manufacture:

(1) Serially connected dual-grating fibers with different wavelengths were selected, and the distance between these two gratings was 10mm. During manufacture, a non-metal loose sleeve and a metal capillary were used to package these two grating fibers, respectively. Before encapsulation, a wire stripper was employed to strip a small part of the coating layer at both ends of the grating, which was then wiped clean. The selected sleeve was applied while maintaining the grating in a tensioned state. Finally, epoxy was used to secure the gratings at the point where the sleeve port contacts the optical fiber.

(2) A steel bolt was selected for subsequent secondary processing. The bolt has a length of 400 mm

and a diameter of 14 mm. An axial groove, 2 mm wide and 2 mm deep, was set on the surface of the bolt, and the groove was cleaned with alcohol.

(3) A pretensioning method was adopted to maintain a certain level of prestress in the optical fiber. The FBG sensor was affixed and encapsulated in the axial groove using an epoxy resin binder, ensuring the binder filled the groove without forming bubbles. The tail fiber was drawn from the end of the bolt rod for further encapsulation and protection.

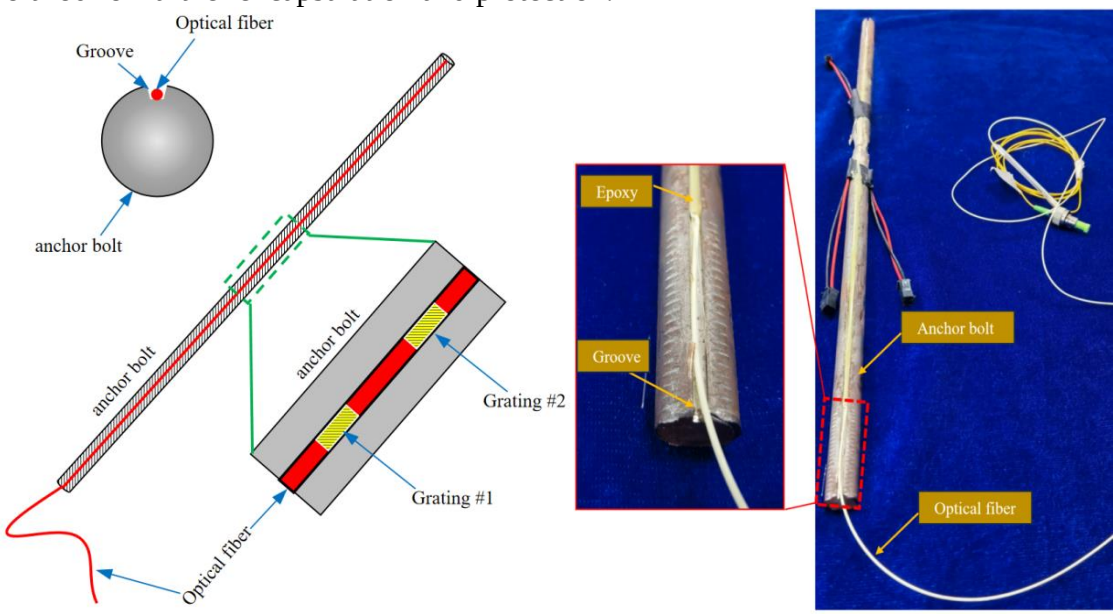

Figure 1: Schematic diagram and photo of developed dual grating embedded bolt.

The double grating fiber was packaged in the bolt rod's groove to protect the fiber grating from damage in harsh construction environments. Simultaneously, the temperature sensitivity coefficient and the strain sensitivity coefficient of the grating were differentiated to achieve temperature compensation. The fabricated double-grating fiber sensor is illustrated in Figure 1.

4. Experimental investigation on the sensing performance

In this study, six prototypes were fabricated in the laboratory to investigate the temperature and strain sensing performance of the developed anchor equipped with temperature-compensated double-grating fibers. Details of the grating wavelength and the materials used for the seal casing are provided in Table 1.

A cross-sensing test was conducted on these six bolts to verify the sensing performance of the developed steel bolts and to investigate whether the temperature and strain can be effectively decoupled to achieve temperature compensation. The sensitivity coefficients calibrated in the previous experimental investigation as shown in Table 1 were utilized for data analysis. The program-controlled universal testing machine WHSD-150kN was employed during this test to apply tension. A temperature control belt and a temperature sensor were wrapped around the anchor rod to regulate and measure temperature. The setup for this test is illustrated in Figure 2. Additionally, three different sets of ambient temperatures (25/35/45℃) and tension strains (400/800/1200με) were established for the test.

Table 1: Temperature/strain sensitivity coefficients of the grating after tube package

Optical fiber		Grating wavelength /nm	Temperature sensitivity coefficient pm/ ℃	Strain sensitivity coefficient pm/με	$K_{T1}K_{\varepsilon 2} - K_{T2}K_{\varepsilon 1}$
#1	Bare gate #1-1	1556	21.44	1.34	-6.88
	Steel capillary #1-2	1550	23.19	1.13	
#2	Bare gate #2-1	1556	22.63	1.29	-8.42
	Steel capillary #2-2	1550	25.78	1.10	
#3	Bare gate #3-1	1542	18.02	1.33	-14.38
	Steel capillary #3-2	1546	25.32	0.95	
#4	Bare gate #4-1	1556	22.57	1.07	-7.62
	Loose casing #4-2	1550	28.06	1.00	
#5	Bare gate #5-1	1550	15.15	1.09	-2.33
	Loose sleeve #5-2	1556	16.92	1.06	
#6	Bare gate #6-1	1548	22.71	0.94	0.09
	Loose casing #6-2	1550	22.33	0.92	

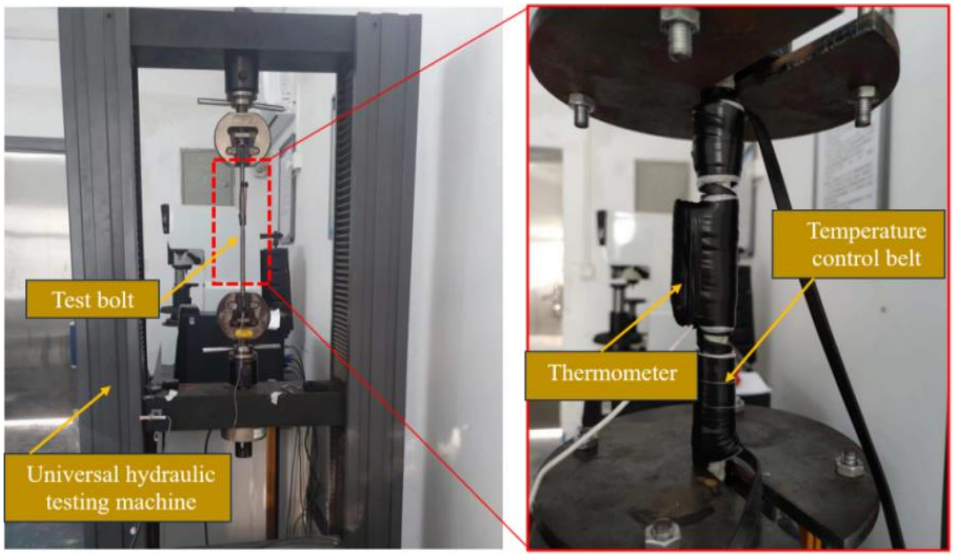

Figure 2: Setup of sensing test device.

During the investigation, each of the six bolt samples was tested individually, yielding nine sets of data per sample, which included both wavelength and strain measurements for each bolt. Utilizing the wavelength $\Delta\lambda_1 / \Delta\lambda_2$ under varying temperature and strain testing conditions, the temperature change ΔT and strain change $\Delta\varepsilon$ can be were calculated. These calculations were based on the double grating temperature compensation method and the sensitivity coefficients of the bolts, as calibrated and listed in Table 1.

The experimental results allow for the analysis of various scenarios where the temperature change ΔT equals 0, 10, or 20 ℃, and the strain change measured by the strain gauge $\Delta\varepsilon$ equals 0, 400, or 800 με. This paper selects the data group with the largest changes, which effectively represents simultaneous changes in temperature and strain. This group also exhibits a significant wavelength difference, yielding more robust data analysis results. Specifically, the wavelength data corresponding to a temperature change $\Delta T = 10$ ℃ measured by the thermometer and a strain change $\Delta\varepsilon = 800$ με measured by the strain gauge were analyzed. The results are presented in Table

2.

Table 2: Change of grating wavelength in six bolts at $\Delta T = 10℃$ and $\Delta\varepsilon = 800\mu\varepsilon$

Number of bolts	$\Delta\lambda_1$	$\Delta\lambda_2$	ΔT	Δε	ΔT Calculation error (%)	Δε Calculation error (%)
#1	1305	1156	11.04	797.38	10.44	0.33
#2	1275	1140	8.38	838.75	16.22	4.84
#3	1239	1017	10.75	787.07	7.47	1.62
#4	1070	1081	12.30	737.59	23.00	7.80
#5	1017	1020	13.12	752.01	31.22	6.00
#6	980	992	8.51	842.03	14.88	5.25

If ignoring the influence of temperature change, *i.e.*, the temperature compensation is not carried out, thus the strain change $\Delta\varepsilon$ can be calculated as shown in Table 3. The error of the strain variation is between 17% and 35%.

Table 3: Strain variation calculated without temperature compensation Δε

Number of bolts	$\Delta\lambda_1$	$\Delta\lambda_2$	$\Delta\varepsilon_1$	$\Delta\varepsilon_2$	$\Delta\varepsilon_1$ Calculation error (%)	$\Delta\varepsilon_2$ Calculation error (%)
#1	1305	1156	974.10	1024.37	22	28
#2	1275	1140	985.24	1034.76	23	29
#3	1239	1017	932.91	1074.60	17	34
#4	1070	1081	996.00	1083.49	24	35
#5	1017	1020	934.74	961.27	17	20
#6	980	992	1047.57	1074.17	31	34

As shown in Table 2, the solving error Δε for bolts #1 through #6 is less than 5%, indicating that these values are closer to the actual strain measurements than those calculated without temperature compensation, as listed in Table 3.

As shown in the calibrated sensitivity coefficient results in Table 1, the temperature sensitivity coefficient and strain sensitivity coefficient for bolts #5 and #6 are similar, resulting in the ratio *i.e.*, $K_{T1}K_{\varepsilon 2} - K_{T2}K_{\varepsilon 1}$, being very close to 0. It is known that a greater discrepancy between the temperature sensitivity coefficient and the strain sensitivity coefficient enhances the conditions required for the dual-wavelength matrix method, *i.e.*, $K_{T1}/K_{T2} \neq K_{\varepsilon 1}/K_{\varepsilon 2}$, and improves the decoupling performance of strain and temperature values. Consequently, for bolt #5 and #6, during the matrix calculation process, even a small fluctuation in wavelength can cause a significant error ΔT and $\Delta\varepsilon$ in the calculated values.

Thus, compared to anchor rods #1, #2, and #3, which are packaged with capillary steel tubes, the sensitivity coefficient of those packaged with loose casing exhibits instability. Therefore, it can be concluded that capillary steel tube packaging is more conducive to measuring strain in the temperature-compensated dual-grating anchor bolt embedded in the surrounding rock.

5. Conclusion

Drawing on the principles of the dual-wavelength matrix method, this study introduces a method for tube encapsulation of double grating, thereby modifying the temperature and strain sensitivity coefficients to obtain double gratings with distinct coefficients. Moreover, a novel

temperature-compensated anchor bolt was developed in conjunction with the steel bolt, and its cross-sensing performance was rigorously tested. Key findings and contributions of this research include: the structure of a smart bolt incorporating double grating temperature compensation was designed. In addition, a theoretical dual-wavelength matrix method was established for the decoupling formula of temperature and strain, analyzing the impact of the sensitivity coefficient of double grating on the decoupling outcome.

In summary, this study designed and developed a temperature-compensated dual-grating anchor bolt to reinforce structures such as masonry and concrete. This innovation provides a robust technical foundation for establishing a stability evaluation system that conducts real-time safety monitoring, issues early warnings of potential disasters, and effectively reduces accidents.

Acknowledgments

This work was supported by the Special Fund of Hubei Safety Production Science and Technology Project, Hubei Emergency Department (Grant number: Hubei Emergency Office [2022] No.12), Key technology research and application of intelligent anchor-based mine roadway rock support and ground pressure deformation monitoring. The authors would like to thank for them for their financial support.

References

[1] Wu C. (2018) Application of bolt support and reinforcement technology in mine roadway excavation. Technology and Market, 25(08), 116+118.

[2] Chu L. (2021) Application of bolt support technology in mine roadway excavation. World Nonferrous Metals, 17,231-232.

[3] Pan W., He C., Wu F., Fu J., and Yang W. (2023) Study on advanced support and anchor directional pre-rein for cement of layered soft rock tunnel. Chinese Journal of Underground Space and Engineering, 19(2), 1-15.

[4] Gao H. and Mei Y. (2022) Anchoring experiment and intelligent optimization algorithm for mountain tunnel bolt. Journal of Intelligent Building and Intelligent City, 7, 158-160.

[5] Jin F. and Lu N. (2022) Research on slope support technology in construction. China Construction, 10,137-138.

[6] Hu H. (2022) Research on the application of slope support technology in civil engineering. Technology Application, 17,140-142.

[7] Chai J., Lan S., LI J., Li Y. and Liu J. (2005) Stree-strain monitoring system of fiber bragg grating sensing for mining anchor. Journal of Xi 'an University of Science and Technology, 1, 1-4.

[8] Jiang D., Zuo J., Xin S., Liang L., and Nan Q. (2005) Application of FBG sensor on anchor rod in project Shuibuya. Journal of Transducer Technology, 1, 72-74.

[9] Liang M., Fang X., Chen N., Ma M., and Li X. (2018) Strain sensing mechanism of surface bonded fiber Bragg grating bolt and its application. Journal of China University of Mining and Technology, 47 (6), 1243-1251.

[10] Chen J., Ding Y., Zhou K., Li L., and Cheng H. (2016) Research and application of FBG bolt stree meter in tunnel safety monitoring. Geotechnical Investigation and Surveying, 44(12), 48-51.

[11] Dong J., Xie Z., Yang E., and Zheng G. (2021) Monitoring and analysis of the bolt supporting for the mining roadways based on the FBG sensor. Journal of Safety and environment, 21(5), 2013-2021.

[12] Liu J. (2016) Study of dynamic monitoring technology with temperature compensation for the Fiber Bragg grating bolt stress. Coal Mine Mechanical and Electrical, 3,33-37 + 41.

[13] Tian S., Zhao X., Ou J., Zhou Z. and Wan L. (2002) Research on temperature compensation of Fiber Bragg grating for Structural Health Monitoring. Journal of Transducer Technology, 12, 8-10.